Journal of Materials Chemistry A

ROYAL SOCIETY OF CHEMISTRY

PERSPECTIVE

View Article Online
View Journal | View Issue

Cite this: J. Mater. Chem. A, 2022, 10, 19552

Introducing porosity into metal–organic framework glasses

Lauren N. McHugh * and Thomas D. Bennett *

Received 6th April 2022
Accepted 12th June 2022

DOI: 10.1039/d2ta02560d

rsc.li/materials-a

Glasses formed by the melt quenching of metal–organic frameworks (MOFs) are the first new category of glass since metallics in the 1970s, and have begun to redistribute attention in the MOF field away from the crystalline state. Those formed to date are, however, relatively dense and so proposed interest focuses mainly on their physical properties. Here, we suggest routes to incorporate porosity into the glasses, borrowing from both inorganic and organic polymer science. We then speculate on the future adsorptive applications of these materials.

Introduction

Metal–organic frameworks (MOFs) are hybrid materials, consisting of a three-dimensional (3D) network of inorganic metal ions or clusters and organic connecting linkers.[1] The cage-like structures of MOFs can lead to the presence of cavities or 'pores' within the materials, which allow the selective adsorption of guest molecules. Their adsorptive properties have led to proposed uses in applications ranging from gas adsorption and separation,[2–4] to catalysis[5] and sensing.[6]

Glasses are 'frozen liquids', produced mainly by rapid cooling of a liquid to form a disordered solid state. In addition to the three previously known categories of glasses: inorganic, organic and metallic, a fourth category known as 'hybrid' glasses was recently discovered. The first examples of these hybrid glasses were formed from a class of MOFs called zeolitic imidazolate frameworks (ZIFs). ZIFs are composed of tetrahedrally-coordinated metal ions and imidazolate linkers,[7–9] with metal-imidazolate-metal bond angles close to the 145° Si–O–Si angle observed in aluminosilicate zeolites.

Various ZIFs have been shown to form glasses *via* melt-quenching,[10–12] with structures similar to that of amorphous silica, *i.e.* with a continuous random network of tetrahedrally-

Department of Materials Science & Metallurgy, University of Cambridge, 27 Charles Babbage Road, Cambridge, CB3 0FS, UK. E-mail: lnm30@cam.ac.uk

Tom was awarded his PhD in 2012 at the University of Cambridge, where he worked with Professor Anthony Cheetham FRS on the physical properties of hybrid frameworks. He has received several fellowships and awards, including a Royal Society Research Fellowship (2016), the Woldemar A. Weyl award for glass science (2019), the Philip Leverhulme Prize in Chemistry (2019), the Royal Society of Chemistry Harrison Meldola Memorial Prize (2020) and the Chemical Communications Lectureship (2021). He has held visiting positions at the University of Kyoto, the Wuhan University of Technology, and the University of Canterbury New Zealand|Te Whare Wānanga o Waitaha. He is vice-chair of the international MOF advisory committee, and outgoing chair of the Royal Society of Chemistry Porous Materials Group. He is currently an Assistant Professor at the University of Cambridge, where his research group are best known for the discovery of hybrid melt-quenched glasses, and seminal works exploring the interface of the coordination polymer, MOF and glass domains. Find out more about Tom and his group (https://tdbennettgroup.com/, @thomasdbennett).

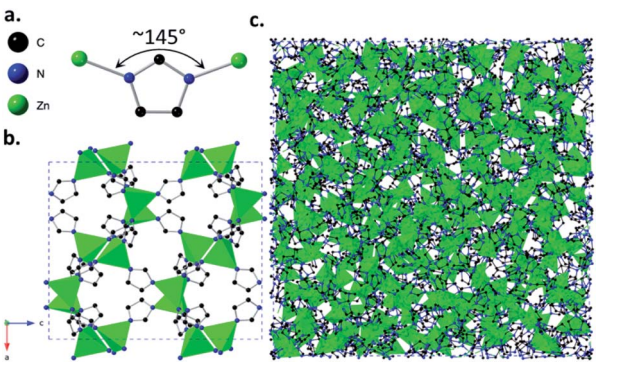

Fig. 1 (a) Zn-Im-Zn angle of ZIF-4(Zn) [$Zn(Im)_2$] structural unit, (b) crystalline structure of ZIF-4(Zn) with unit cell parameters a = 15.3486(14), b = 15.1069(17), c = 18.3430(19), *Pbca*, **cag** topology, (c) atomic configuration of melt-quenched a_gZIF-4(Zn), where a_g denotes the glass phase. Configuration parameters: $a = b = c$ = 47.5225 Å, *P1*. CIFs obtained from ref. 9 and 11 respectively.

coordinated Zn^{2+} ions and imidazolate linkers.[13] Glass forming ZIFs include the imidazolate-based ZIF-4(Zn) ($[Zn(Im)_2]$, Im = imidazolate, $[C_3H_3N_2^-]$) (Fig. 1) and the mixed-linker ZIF-62(Zn) ($[Zn(Im)_{2-x}(bIm)_x]$, bIm = benzimidazolate, $[C_7H_5N_2^-]$). Research into ZIF glasses has thus far highlighted their mechanical and optical properties,[14,15] and preliminary studies into their adsorptive properties have shown features such as their ability to separate hydrocarbons and other mixtures of chemicals from one another.[16,17]

This article explores porosity in crystalline MOFs and how this is affected upon glass formation. Current methods used in glass science to increase porosity will then be covered, followed by consideration of how they may in future be used to impart MOF glasses with porosity. We will then speculate on the prospective adsorptive applications of such porous MOF glasses, and in particular, how they may offer significant promise in environmental remediation applications.

Discussion

Porosity in crystalline MOFs

A fundamental feature of MOFs is their porosity, with larger pores typically leading to higher reported surface areas and subsequently, greater promise in adsorption-based applications. In the two decades since their discovery, MOFs with increasingly higher porosities have been reported. This has been linked to the use of isoreticular chemistry, which involves increasing the length of the organic connecting linker, to allow pore-size tailoring and the formation of larger and larger pore cavities. The concept of isoreticular MOFs (IRMOFs) was first reported by Eddaoudi *et al.*, where octahedral ZnO clusters are connected to linkers with the same linear geometry, though different lengths. Examples of which include IRMOF-1 (bdc, 1,4-benzenedicarboxylate, $[C_8H_4O_4^{2-}]$) and IRMOF-16 (tpdc, *p*-Terphenyl-4,4″-dicarboxylate, $[C_{20}H_{12}O_4^{2-}]$), where in some cases, mesopores of greater than 20 Å are reported.[18]

A further well-known series of highly porous IRMOFs includes the Zr_6 cluster based UiO series reported by Cavka *et al.*, which include the exceptionally stable UiO-66(Zr), UiO-67(Zr) and UiO-68(Zr).[19] Other examples of large-pore and high surface area MOFs include NU-1501-Al, reported by Chen *et al.*, which displays pores ranging from 15–25 Å and a Brunauer–Emmett–Teller (BET) surface area of 7310 $m^2\ g^{-1}$.[20] The current "record" BET surface area is attributed to DUT-60, first reported by Hönicke *et al.* DUT-60 reports a BET surface area of 7839 $m^2\ g^{-1}$, and mesopores with dimensions of up to 37 × 42 Å are observed.[21]

Existing porosity in amorphous MOFs and MOF glasses

Upon the amorphisation of crystalline MOFs, either by the application of pressure or by heat-treatment, the accessible porosity is typically reduced. The reduction in porosity within pressure-amorphised ZIF-8(Zn) ($[Zn(mIm)_2]$, mIm = 2-methyl imidazolate, $[C_4H_5N_2^-]$) samples is highlighted by Chapman *et al.*, and shows crystalline samples exposed to differing levels of nonhydrostatic pressure. The resultant BET surface areas reduce with increasing applied pressure, and a reduction in pore volume is observed, with pressure-induced pore modification evident.[22] Further investigation of pressure-assisted pore collapse includes the larger-pore MOF, UiO-66(Zr). Here, Su *et al.* show that Zr–O bonds between clusters and bridging linkers break upon the application of pressure, once again leading to an effectively non-porous sample with very low pore volume.[23]

The stepwise collapse of pore structures within MOFs upon mechanical milling is highlighted by Sapnik *et al.* and shows that the highly porous MIL-100(Fe) is mechanically amorphised in a vibratory ball-mill. The resultant amorphous MIL-100(Fe) is effectively non-porous to nitrogen (N_2), showing a collapse of the porous interior (Fig. 2a).[24]

This reduction in porosity is also apparent upon the formation of melt-quenched MOF glasses from their parent crystalline forms, where the accessible porosity is reduced, and the framework becomes significantly denser. Discussions of porosity within MOF glasses are somewhat limited, due both to the infancy of the field, and the difficulty in determining porosity using standard experiments. The typical experimental determination of porosity within porous materials uses a probe gas such as N_2 to find the accessible surface area and subsequent pore size. The relatively dense structure of MOF glasses, however, means that their porosity is typically much lower, and this form of analysis is therefore not always possible.

The first report of MOF glasses by Bennett *et al.* highlights that they are essentially non-porous to N_2, with a_gZIF-4(Zn) reporting a BET surface area of <5 $m^2\ g^{-1}$.[25] Due to this low porosity, in some cases, a non-destructive technique known as 'positron annihilation lifetime spectroscopy' (PALS) may also be used to determine the internal porosity. This form of analysis is used in the study of porosity within several ZIF glasses by

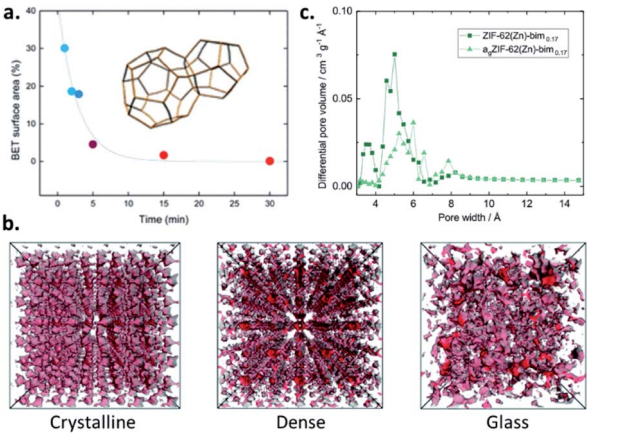

Fig. 2 (a) Decrease in the BET surface areas of MIL-100(Fe) with increasing milling time due to pore collapse (reproduced from ref. 24 with permission from the Royal Society of Chemistry), (b) accessible porosity using a probe 1 Å in diameter of the crystalline, dense and glass forms of ZIF-4(Zn) from PALS data (reproduced from ref. 26 with permission from the Royal Society of Chemistry), (c) pore size distribution of a_gZIF-62(Zn) (bIm = 0.17) (reprinted with permission from ref. 16. Copyright 2019 American Chemical Society).

Thornton *et al.*, including crystalline ZIF-4(Zn) and its two dense forms with identical chemical composition: ZIF-zni(Zn) and a_gZIF-4(Zn) (Fig. 2b). a_gZIF-4(Zn) displays both the smallest and largest pore sizes, with cavities estimated as 6.9 Å and 2.6 Å. Comparable analysis with crystalline ZIF-4(Zn) estimates pores with diameters of 6.2 Å and 3.3 Å, while the dense phase ZIF-zni(Zn) presents pore sizes of 6.6 and 3.8 Å. It should, however, be emphasised that PALS can overestimate the pore sizes compared to those determined from computational analysis. While the results are somewhat comparable for a_gZIF-4(Zn), considerable overestimations in the pore dimensions in the crystalline phases are evident.[26]

Further investigation into ZIF-4(Zn) includes computational analysis of the 'liquid' state of the material, which is formed upon the melting of crystalline ZIF-4(Zn), though prior to glass formation. Gaillac *et al.* show that the porosity of the parent crystalline state is preserved in the liquid state of ZIF-4(Zn), though this is observed to be transient in nature. This pore volume is greater than that of the glass form, suggesting a partial collapse of the pore structure upon quenching.[11] While the simulations by Gaillac *et al.* do indeed provide further clarity on the crucial intermediate liquid phase of ZIF-4(Zn), and are overall in good agreement with experimental studies, they do neglect some crucial details known from experimental work. These include the metastability of the ZIF-4(Zn) liquid, a polymorphic low to high density transition after melting, and rapid recrystallisation of the liquid to the much denser zni topology polymorph. The zni polymorph melts at a much higher temperature, forming a glass upon quenching.

In addition to PALS and computational methods, probe gases with a lower kinetic diameter than N_2, such as carbon dioxide (CO_2) may in some cases be used to experimentally determine the adsorptive properties of MOF glasses. This method has been used in the investigation of the adsorptive properties of one of the most extensively studied MOF glasses: the mixed linker a_gZIF-62(Zn).

CO_2 gas adsorption is used in the experimental determination of the permanent porosity within a_gZIF-62(Zn). Widmer *et al.* state that the material reversibly adsorbs 0.90 mmol g^{-1} STP, and that the uptake of the glass is around half that of crystalline ZIF-62(Zn), which adsorbs 1.74 mmol g^{-1} STP. Both forms of ZIF-62(Zn) are non-porous to N_2, though display low levels of porosity to H_2 and extremely low porosity to O_2.[27]

Further investigation into the adsorptive properties of a_gZIF-62 involves the cobalt-version of ZIF-62 glass: a_gZIF-62(Co). Frentzel-Beyme *et al.* show that, like its zinc equivalent, a_gZIF-62(Co) also displays porosity to CO_2, and again adsorbs approximately half the amount adsorbed by crystalline ZIF-62(Co) (0.75 v 1.65 mmol g^{-1} at 95 kPa).[28]

Nonlocal density functional theory (NLDFT) of CO_2 isotherms may be used to determine specific surface areas and pore size distributions. This method is used by Frentzel-Beyme *et al.* to further investigate the adsorptive properties of both glass and crystalline ZIF-62(Zn) with varying bIm ratios, where a_gZIF-62(Zn)-bIm$_x$ again displays surface areas around half those of the corresponding crystalline ZIFs (235–269 m^2 g^{-1} v 439–504 m^2 g^{-1}). Pore size distributions reveal the almost complete loss of small pores (those with diameter ~3.5 Å), though significant preservation of medium pores (5–6 Å) and formation of some larger cavities (~8 Å) is observed upon formation of a_gZIF-62(Zn)-bim$_x$ (Fig. 2c).

Very recent work by Frentzel-Beyme *et al.* has since provided further understanding of the existing porosity in MOF glasses, by quantifying the gas-accessible microporosity available in those glasses identified to date. CO_2 gas adsorption conducted at 195 K allows experiments to reach saturation, hence enabling the accurate determination of specific pore volumes. The authors also suggest that current methods used to determine the pore size distributions in MOFs glasses, *i.e.* NLDFT and Horvath–Kawazoe (HK) are inadequate, and that improvements are required in future statistical models based on CO_2 adsorption to more accurately reproduce the porosity within MOF glasses.[29]

Excitingly, and for the first time, a_gZIF-62(Zn) is shown to be porous towards larger hydrocarbon gases, such as *n*-butane, propane, and propylene. The larger kinetic diameter of *n*-butane (4.3 Å) compared to CO_2 (3.3. Å) leads to significant hysteresis upon desorption, suggesting a limitation on diffusion out of the pores. Subsequent investigation concentrates on the adsorption and separation of the technologically relevant hydrocarbons propane and propylene, where all the glasses show a preference for the adsorption of propylene over propane and a thermodynamic propene/propane selectivity between 1.8 and 2.5 (for a 1 : 1 mixture) for the ZIF glasses.[16]

Methods for increasing porosity in existing glasses

Porous inorganic glass samples have been formed by many methods, including 'salt sintering' by Liang *et al.*, where borate glass ($Na_2O \cdot CaO \cdot B_2O_3$) is mixed with sodium chloride, then pelletised and heated, before dissolution of the salt in water to provide a highly porous material.[30] Other techniques used to produce porous glasses include the two-stage solution-gelation (sol–gel) process. The first stage (sol) involves the conversion of precursors into a colloidal solution, typically *via* controlled hydrolysis. This is followed by an acid or base catalysed polycondensation reaction (gel). The process results in a rigid and highly interconnected 3D network. The technique has been applied to a variety of glasses, including silica glasses by Santos *et al.*,[31] and bioactive glasses by Deshmukh *et al.*[32]

Other techniques include metastable phase separation in silicate glasses, highlighted by Suzuki and Tanaka. The method involves the decomposition of a single glass phase into two or more phases upon heat-treatment. Certain phases have 3D interconnected microstructures and are obtained by acid leaching, to form a highly porous glass.[33] This phase separation technique is used to produce the well-known and commercialised porous inorganic glass: Corning Vycor® 7930 Porous Glass, developed by Corning Incorporated. The glass has the colloquial name 'thirsty glass' due to its excellent moisture adsorbing properties and displays very good thermal shock resistance and optical quality. The predominantly silica-based mesoporous glass contains small amounts of diboron trioxide (B_2O_3)

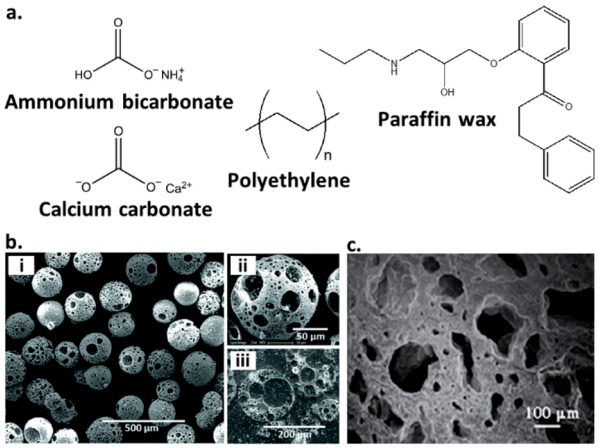

Fig. 3 (a) Structures of selected inorganic and polymeric porogens used to imbue inorganic glasses with porosity, (b) (i and ii) SEM images at increasing magnification of a porous borate glass microsphere produced using calcium carbonate as a porogen, (iii) cross-sectional SEM image showing the fully interconnected pores (reproduced from ref. 35 with permission from the Royal Society of Chemistry), (c) SEM image of a silica-based glass ceramic scaffold produced using polyethylene as a porogen. A mixture of macropores and diffuse micropores are observed and clear pore interconnectivity is evident (reprinted by permission from Springer Nature: Journal of Materials Science: Materials in Medicine, ref. 36, copyright 2007).

and sodium oxide (Na_2O), with an average pore diameter of 40 Å.[34]

Another common route to the preparation of porous inorganic glasses includes the use of chemicals known as 'porogens', which are particles of specified shape and size that decompose within a glass and imbue porosity within it (Fig. 3a). Examples of the use of porogens include the production of highly porous glass scaffolds by Erasmus *et al.*, which are promising materials in the fabrication of bone replacements. Production involves mixing pre-synthesised borosilicate, borophosphate and phosphate bioactive glasses with the foaming agent: ammonium bicarbonate at weight percentages of 60 and 70%. The salt is then 'burned out' to provide a highly porous material, before the glasses are sintered at high temperature. This produces strong, porous glass scaffolds with porosity >50% and interconnected pores in the range of 250–570 μm.[37] Another example is the formation of highly porous borate glass microspheres by M. Islam *et al.* Samples with porosity of 65–75% and pore sizes of 43–52 μm are produced using calcium carbonate as a porogen (Fig. 3b).[35]

Other examples of porogens are polymeric fillers, which are removed *via* heat treatment prior to sintering. These include polyethylene (PE) powders of varying size ranges and incorporated at 25–70 vol%, used by Brovarone *et al.* to produce bioactive silica-based glass ceramics. The resultant glass scaffolds contain highly interconnected pores, and depending on the amount and size of PE powders, macropores of up to 500 μm and porosities of 50–70% are achievable, with uniformly dispersed microporosity also evident (Fig. 3c).[36]

Further studies involving polymeric fillers include the use of paraffin wax by Zhang *et al.*, where differing ratios of powdered paraffin wax result in highly porous apatite/wollastonite bioactive glass ceramic scaffolds with interconnected porosity of up to 70%, and macropores of 250–350 μm.[38]

Unlike porous inorganic glasses, porous organic glasses are not typically formed *via* post-synthetic modification of an existing glass and are instead produced directly from organic precursors. Examples include those produced from porous organic cages by Brand *et al.*, where the glasses are formed from melt-quenching *via* the liquid state. While they display low BET surface areas, their CO_2 and methane (CH_4) uptakes are similar to ZIF glasses.[39] Other examples of porous organic glassy materials are polymers of intrinsic microporosity (PIMs), first reported by Budd *et al.*, which are amorphous, nanoporous organic materials with pore sizes in the range of 5.2 to 10.7 Å.[40–42] The porosity within PIMs is intrinsic in nature, and results from the inefficient packing of their rigid and contorted macromolecular chains. PIMs are typically formed by polymerisation reactions involving the formation of dibenzodioxin, Troger's base, or imide linkages.[43]

Imbuing MOF glasses with porosity

As discussed previously, MOF glasses do display some permanent, accessible porosity to small molecules, though their overall porosities are low. This poses problems with the future applicability of MOF glasses, especially their use in the adsorptive applications their crystalline counterparts are so well known for. MOF glasses objectively offer an exciting alternative to crystalline MOFs in some respects, due to their increased mechanical stability and grain-boundary free nature. This means that processing the materials into useable forms is in theory easier. Increasing, or 'tuning' the porosity within MOF glasses, while also utilising the increased durability of the glass phase, would lead to a potentially transformative new family of functional adsorptive materials, for use in a wide range of adsorptive applications.

Techniques used to increase the pore size in crystalline MOFs, such as isoreticular chemistry, are likely to be less transferrable to MOF glasses. While the initial MOF may be highly porous, much of the porosity will be lost due to the densification of the framework upon glass formation. In addition, most isoreticular MOFs are carboxylate-based, which typically decompose upon heat-treatment, rather than melt and form glasses.[44] Whilst an isoreticular extension of ZIFs *i.e.* in the same way as carboxylate-based MOFs is perhaps not possible due to the specific coordination geometry in ZIFs, the use of *e.g.* Bisimidazolate ligands may well lead to a family of Metal Azolate glass formers with improved porosity. It does, however, remain unclear whether the high thermal stabilities observed in current members of the ZIF family would be retained in such variants.

Techniques used in traditional glass science to imbue samples with porosity may be much more transferrable to MOF glasses, and while post-synthetic modification of pre-synthesised glass samples may be possible, instilling porosity into MOF glasses is most likely to be achieved by the decomposition of chemicals added during glass formation. One

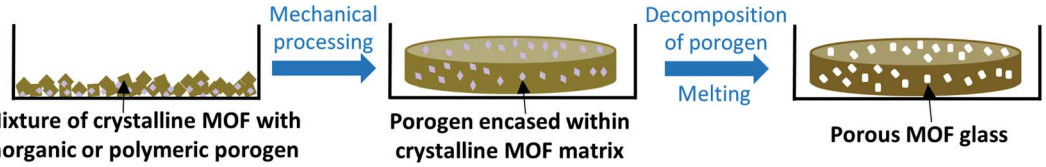

Fig. 4 Proposed formation of porous MOF glasses *via* the decomposition of inorganic or polymeric porogens.

promising route may involve the use of porogens similar to those used in glass science *i.e.*, inorganic or organic species which decompose upon heating, or particles such as polymers, which may degrade upon the exposure of external stimuli such as UV light (Fig. 4).[45] Other possibilities to produce porous MOF glasses may borrow from the production of PIMs, which involves the controlled packing of organic molecules. Careful consideration of MOF subunits may allow the design of MOF glasses with intrinsic porosity.

The formation of MOF glasses from their corresponding crystalline phase typically results in a reduction in gas adsorption capability and pore size, though an increase in sorption capacity is observed for so called MOF crystal-glass composites (MOF-CGCs), where the crystalline phase of a MOF is stabilised within a glass phase. First demonstrated by Hou *et al.*, the open pore phase of MIL-53(Al) [Al(OH)(bdc)] is stabilised within an a_gZIF-62(Zn) matrix.[46]

A further study by Ashling *et al.* on MOF-CGCs showed that the MOF-CGCs adsorb significantly higher quantities of CO_2 at high MOF loading than the narrow-pore phase of the MOF alone.[47] Ashling *et al.* also highlighted that limitations in the gas uptake in further examples are, however, largely dominated by the glass matrix, and to improve the porosity of the MOF-CGCs, the glass matrix porosity must also be enhanced.[48] McHugh *et al.* then showed that MOF-CGCs produced from crystalline and glass phases of the same MOF show good interfacial compatibility between the two phases. These composites perhaps offer greater tuneability and applicability than standard MOF-CGCs, though their adsorptive capability is again limited by the low porosity of the base MOF glass.[49]

The use of porogens with different particle sizes would allow the tuneable formation of a wide range of pore sizes within MOF glasses, even the smallest pores lost upon glass formation, to provide adsorptive materials which may be tailored to specific adsorptive applications.

Proposed applications

One of the most noteworthy potential applications of such porous MOF glasses might be their use in environmental remediation applications, such as their use as chemical separation membranes. The separation of chemicals, including CO_2 removal and the production of clean water, account for 10–15% of the world's energy consumption.

Such procedures are typically performed using highly energy-intensive and polluting processes such as distillation, which contribute significantly towards greenhouse gas emissions. A transition to greener membrane-based separations could reduce energy use by 90% (Fig. 5), preventing the annual emission of 100 million tonnes of CO_2.[50]

While the development of new membrane materials has advanced significantly in recent years, the technology remains somewhat underdeveloped. This is due in part to complicated fabrication procedures, their poor scalability, and their somewhat low thermal and chemical stability.

Membranes derived from crystalline, *i.e.* ordered materials (including MOFs) offer tuneable porosities, high chemical selectivity's and have connected pore structures.[51–54] They are hence highly suited to chemical separation applications, though their low durability typically requires the presence of a porous support for mechanical strength (Fig. 6a). For example, crystalline ZIF-8(Zn) has been used extensively in such membranes. ZIF-8(Zn) crystals are typically grown on porous supports such as rigid alumina by Tran *et al.*,[55] or flexible polypropylene by Zhao *et al.*,[56] and are utilised in the separation of mixtures such as propane and propene. Crystalline ZIF-4(Zn) has also been incorporated into mixed matrix membranes by Hovestadt *et al.*, where the material is dispersed within a polymer matrix, which is then utilised for paraffin and olefin separation.[57]

As discussed previously, recent developments in the characterisation of MOF glasses have highlighted their potential as

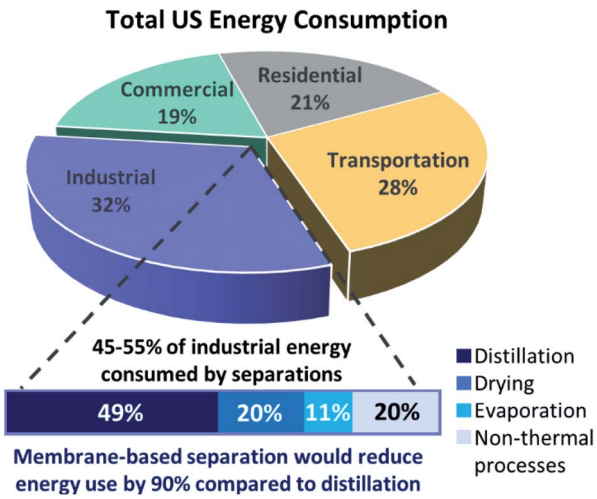

Fig. 5 Schematic of total US energy consumption and how membrane technology would reduce energy usage significantly (adapted by permission from Springer Nature: Nature, ref. 50, copyright 2016).

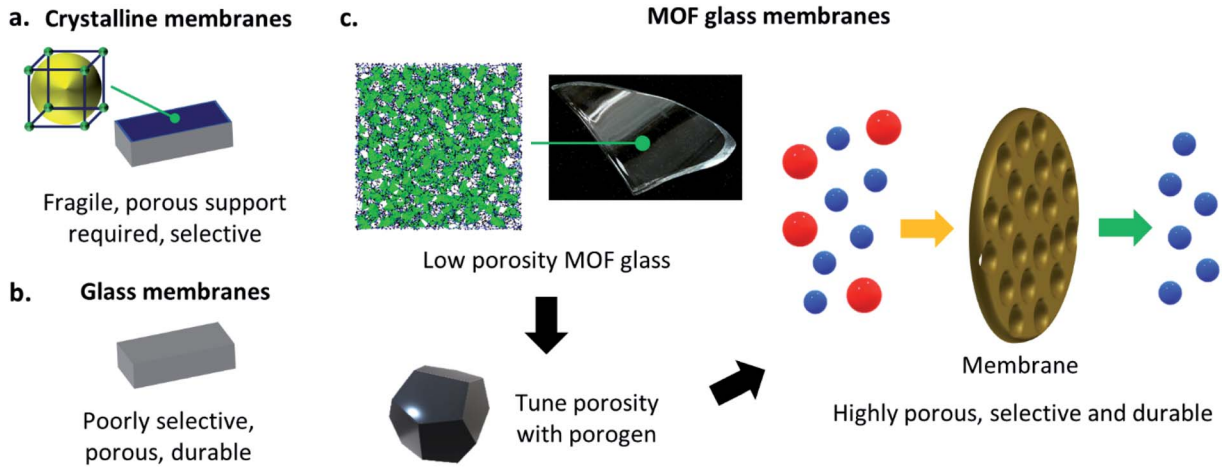

Fig. 6 Schematic of the drawbacks and advantages of (a) crystalline membranes and (b) glass membranes, and (c) the formation of new MOF glass membranes by the introduction of significant porosity into MOF glasses.

chemical separation membranes, due to the retention of some porosity upon vitrification, though like their crystalline counterparts, the glasses still require a porous support at present. Despite the requirement for a support, a recent preliminary study by Wang *et al.* has displayed some exciting results regarding gas separation in MOF glasses. Polycrystalline ZIF-62(Zn) is grown solvothermally on a porous ceramic alumina support, and the polycrystalline membrane is then heat-treated to melt-quench the ZIF-62(Zn) and provide a layer of a_gZIF-62(Zn). During fabrication, the molten layer of ZIF-62(Zn) penetrates the nanopores of the support to eliminate grain boundaries and intercrystalline defects in the resulting glass membrane. The highly stable membrane displays excellent and industrially relevant performance in the separation of gas mixtures including H_2/CH_4, CO_2/N_2 and CO_2/CH_4.[17]

Traditional inorganic or organic polymeric membranes are robust and durable, and hence may not always require the same porous support necessary for crystalline materials such as MOFs, though they are significantly less tuneable (Fig. 6b). The superior mechanical properties of MOF glasses over crystalline MOFs propose the exciting possibility that such porous glass materials might form sufficiently strong membranes that porous supports are no longer needed,[58,59] though strengthening agents such as polymeric binders may offer improved stability if necessary. Rigorous mechanical testing of highly porous forms of MOF glasses would be required to fully investigate the mechanical properties of such membranes, though ideally, they would be synthesisable *in situ* and on a large-scale, without the glass substrates and solvents typically necessary for the casting and fabrication of other examples of self-supporting membranes.[60,61] The resultant porous MOF glass membranes would retain the inherent mechanical stability observed in MOF glasses,[14] and their excellent gas separation selectivity's.[16,17]

Porous MOF glasses with highly tuneable porosity may combine the best of the ordered and disordered world, to provide pioneering new glass membrane materials (Fig. 6c).

Conclusions

The porosity present within crystalline MOFs has made them one of the most promising classes of adsorptive materials to date, though their microcrystallinity means that they typically require processing prior to use. Typically, this is bypassed through forming methods such as pelletisation or sintering, though these are not always easily applicable to MOFs, given their weak mechanical properties.

In recent years, glass forms of MOFs have been produced and these 'hybrid' glasses are only the fourth category of glasses to be discovered. Upon formation of MOF glasses, the inherent porosity so prominent in their crystalline precursors is reduced, and the resultant materials are somewhat dense. While they display interesting physical properties, their adsorptive properties and applications have yet to be explored in depth, though initial research has shown promising results in the separation of selected chemicals.

Porosity in crystalline MOFs is commonly increased *via* the use of extended linkers, and while this approach may not be directly transferrable to thermally stable glass forming ZIFs, related frameworks with improved porosity may be achievable. The thermal stability of such materials and the retention of porosity into the glass phase is, however, unclear.

Techniques used in inorganic glass science to instil porosity into inherently dense samples show particular promise in the formation of porous hybrid glass analogues, and methods such as the use of sacrificial porogens are likely to introduce highly tuneable porosity into samples. Porogens of suitable size may be selected based on the size of pores desired within the MOF glass. The high thermal stabilities of MOF glasses mean that the decomposition of porogens such as inorganic salts and organic polymeric species *via* heat-treatment is a highly plausible method to increase porosity. Methods used to produce porous organic glasses may also be adapted to form hybrid analogues, which might involve the strategic packing of organic molecules.

These highly porous MOF glasses may be studied by a range of experimental techniques, including traditional gas adsorption analysis. The presence of such porosity also offers the opportunity to use a range of other highly specialised experimental methods for studying the porosity of amorphous materials, including small-angle X-ray scattering (SAXS) and small angle neutron scattering (SANS).[62,63]

Porous MOF glasses may be particularly suited to environmental remediation applications, including the separation of industrially relevant chemicals. The glasses could be used to produce innovative, new, and chemically tuneable free-standing membranes, which maintain the high selectivity's observed in MOFs. Due to the increased mechanical stability of MOF glasses over their crystalline precursors, the requirement for the porous support present in current membranes may also be negated. Such membranes might be capable of performing some of the most difficult chemical separations known.

Author contributions

The manuscript was conceptualised and written by L. N. M and T. D. B.

Conflicts of interest

There are no conflicts to declare.

Acknowledgements

T. D. B. thanks the Royal Society for a university research fellowship (URF\R\211013). T. D. B and L. N. M. thank the Leverhulme Trust for a Philip Leverhulme Prize (2019).

References

1 H.-C. Zhou, J. R. Long and O. M. Yaghi, *Chem. Rev.*, 2012, **112**, 673–674.
2 K. Sumida, D. L. Rogow, J. A. Mason, T. M. McDonald, E. D. Bloch, Z. R. Herm, T. H. Bae and J. R. Long, *Chem. Rev.*, 2012, **112**, 724–781.
3 R. B. Lin, S. Xiang, H. Xing, W. Zhou and B. Chen, *Coord. Chem. Rev.*, 2019, **378**, 87–103.
4 S. Hiraide, Y. Sakanaka, H. Kajiro, S. Kawaguchi, M. T. Miyahara and H. Tanaka, *Nat. Commun.*, 2020, **11**, 4–17.
5 M. C. Wasson, C. T. Buru, Z. Chen, T. Islamoglu and O. K. Farha, *Appl. Catal., A*, 2019, **586**, 117214.
6 Y. Zhang, S. Yuan, G. Day, X. Wang, X. Yang and H. C. Zhou, *Coord. Chem. Rev.*, 2018, **354**, 28–45.
7 K. S. Park, Z. Ni, A. P. Côté, J. Y. Choi, R. Huang, F. J. Uribe-Romo, H. K. Chae, M. O'Keeffe and O. M. Yaghi, *Proc. Natl. Acad. Sci. U. S. A.*, 2006, **103**, 10186–10191.
8 Y. Q. Tian, Y. M. Zhao, Z. X. Chen, G. N. Zhang, L. H. Weng and D. Y. Zhao, *Chem. - Eur. J.*, 2007, **13**, 4146–4154.
9 R. Banerjee, A. Phan, B. Wang, C. Knobler, H. Furukawa, M. O'Keeffe and O. M. Yaghi, *Science*, 2008, **319**, 939–943.
10 T. D. Bennett, Y. Yue, P. Li, A. Qiao, H. Tao, N. G. Greaves, T. Richards, G. I. Lampronti, S. A. T. Redfern, F. Blanc, O. K. Farha, J. T. Hupp, A. K. Cheetham and D. A. Keen, *J. Am. Chem. Soc.*, 2016, **138**, 3484–3492.
11 R. Gaillac, P. Pullumbi, K. A. Beyer, K. Chapman, D. A. Keen, T. D. Bennett and F. X. Coudert, *Nat. Mater.*, 2017, **16**, 1149–1154.
12 J. Hou, M. L. Ríos Gómez, A. Krajnc, A. McCaul, S. Li, A. M. Bumstead, A. F. Sapnik, Z. Deng, R. Lin, P. A. Chater, D. S. Keeble, D. A. Keen, D. Appadoo, B. Chan, V. Chen, G. Mali and T. D. Bennett, *J. Am. Chem. Soc.*, 2020, **142**, 3880–3890.
13 T. D. Bennett, A. L. Goodwin, M. T. Dove, D. A. Keen, M. G. Tucker, E. R. Barney, A. K. Soper, E. G. Bithell, J. C. Tan and A. K. Cheetham, *Phys. Rev. Lett.*, 2010, **104**, 2–5.
14 S. Li, R. Limbach, L. Longley, A. A. Shirzadi, J. C. Walmsley, D. N. Johnstone, P. A. Midgley, L. Wondraczek and T. D. Bennett, *J. Am. Chem. Soc.*, 2019, **141**, 1027–1034.
15 A. Qiao, H. Tao, M. P. Carson, S. W. Aldrich, L. M. Thirion, T. D. Bennett, J. C. Mauro and Y. Yue, *Opt. Lett.*, 2019, **44**, 1623.
16 L. Frentzel-Beyme, M. Kloß, P. Kolodzeiski, R. Pallach and S. Henke, *J. Am. Chem. Soc.*, 2019, **141**, 12362–12371.
17 Y. Wang, H. Jin, Q. Ma, K. Mo, H. Mao, A. Feldhoff, X. Cao, Y. Li, F. Pan and Z. Jiang, *Angew. Chem., Int. Ed.*, 2020, **59**, 4365–4369.
18 M. Eddaoudi, J. Kim, N. Rosi, D. Vodak, J. Wachter, M. O'Keeffe and O. M. Yaghi, *Science*, 2002, **295**, 469–472.
19 J. H. Cavka, S. Jakobsen, U. Olsbye, N. Guillou, S. Bordiga, K. P. Lillerud, C. Lamberti, S. Bordiga and K. P. Lillerud, *J. Am. Chem. Soc.*, 2008, **130**, 1–19.
20 Z. Chen, P. Li, R. Anderson, X. Wang, X. Zhang, L. Robison, L. R. Redfern, S. Moribe, T. Islamoglu, D. A. Gómez-Gualdrón, T. Yildirim, J. F. Stoddart and O. K. Farha, *Science*, 2020, **368**, 297–303.
21 I. M. Hönicke, I. Senkovska, V. Bon, I. A. Baburin, N. Bönisch, S. Raschke, J. D. Evans and S. Kaskel, *Angew. Chem., Int. Ed.*, 2018, **57**, 13780–13783.
22 K. W. Chapman, G. J. Halder and P. J. Chupas, *J. Am. Chem. Soc.*, 2009, **131**, 17546–17547.
23 Z. Su, Y. R. Miao, G. Zhang, J. T. Miller and K. S. Suslick, *Chem. Sci.*, 2017, **8**, 8004–8011.
24 A. F. Sapnik, D. N. Johnstone, S. M. Collins, G. Divitini, A. M. Bumstead, C. W. Ashling, P. A. Chater, D. S. Keeble, T. Johnson, D. A. Keen and T. D. Bennett, *Dalton Trans.*, 2021, **50**, 5011–5022.
25 T. D. Bennett, J. C. Tan, Y. Yue, E. Baxter, C. Ducati, N. J. Terrill, H. H. M. Yeung, Z. Zhou, W. Chen, S. Henke, A. K. Cheetham and G. N. Greaves, *Nat. Commun.*, 2015, **6**, 1–7.
26 A. W. Thornton, K. E. Jelfs, K. Konstas, C. M. Doherty, A. J. Hill, A. K. Cheetham and T. D. Bennett, *Chem. Commun.*, 2016, **52**, 3750–3753.
27 R. N. Widmer, G. I. Lampronti, S. Anzellini, R. Gaillac, S. Farsang, C. Zhou, A. M. Belenguer, C. W. Wilson, H. Palmer, A. K. Kleppe, M. T. Wharmby, X. Yu,

S. M. Cohen, S. G. Telfer, S. A. T. Redfern, F. X. Coudert, S. G. MacLeod and T. D. Bennett, *Nat. Mater.*, 2019, **18**, 370–376.
28 L. Frentzel-Beyme, M. Kloß, R. Pallach, S. Salamon, H. Moldenhauer, J. Landers, H. Wende, J. Debus and S. Henke, *J. Mater. Chem. A*, 2019, **7**, 985–990.
29 L. Frentzel-Beyme, P. Kolodzeiski, J.-B. Weiß and S. Henke, *ChemRxiv*, 2021, DOI: **10.26434/chemrxiv-2021-lq308**.
30 W. Liang and C. Rüssel, *J. Mater. Sci.*, 2006, **41**, 3787–3792.
31 A. M. M. Santos and W. L. Vasconcelos, *J. Non-Cryst. Solids*, 2000, **273**, 145–149.
32 K. Deshmukh, T. Kovářík, T. Křenek, D. Docheva, T. Stich and J. Pola, *RSC Adv.*, 2020, **10**, 33782–33835.
33 M. Suzuki and T. Tanaka, *High Temp. Mater. Processes*, 2012, **31**, 323–328.
34 Optica Publishing Group, *Appl. Opt.*, 1979, **18**, 3208–3210.
35 M. T. Islam, L. Macri-Pellizzeri, V. Sottile and I. Ahmed, *Biomater. Sci.*, 2021, **9**, 1826–1844.
36 C. V. Brovarone, E. Verné and P. Appendino, *J. Mater. Sci.: Mater. Med.*, 2006, **17**, 1069–1078.
37 E. P. Erasmus, R. Sule, O. T. Johnson, J. Massera and I. Sigalas, *Sci. Rep.*, 2018, **8**, 1–13.
38 H. Zhang, X. J. Ye and J. S. Li, *Biomed. Mater.*, 2009, **4**, 045007.
39 M. C. Brand, F. Greenwell, R. Clowes, B. D. Egleston, A. Kai, A. I. Cooper, T. D. Bennett and R. L. Greenaway, *J. Mater. Chem. A*, 2021, **9**, 19807–19816.
40 P. M. Budd, B. S. Ghanem, S. Makhseed, N. B. McKeown, K. J. Msayib and C. E. Tattershall, *Chem. Commun.*, 2004, **4**, 230–231.
41 H. Yin, Y. Z. Chua, B. Yang, C. Schick, W. J. Harrison, P. M. Budd, M. Böhning and A. Schönhals, *J. Phys. Chem. Lett.*, 2018, **9**, 2003–2008.
42 A. G. McDermott, G. S. Larsen, P. M. Budd, C. M. Colina and J. Runt, *Macromolecules*, 2011, **44**, 14–16.
43 N. B. McKeown, *Sci. China: Chem.*, 2017, **60**, 1023–1032.
44 C. Healy, K. M. Patil, B. H. Wilson, L. Hermanspahn, N. C. Harvey-Reid, B. I. Howard, C. Kleinjan, J. Kolien, F. Payet, S. G. Telfer, P. E. Kruger and T. D. Bennett, *Coord. Chem. Rev.*, 2020, **419**, 213388.
45 A. K. Tipton, B. G. Lu, P. A. Van Cleemput, M. T. Schulberg, Q. Wu, H. Fu and F. Wang, *US Pat.*, US7208389, 2007.
46 J. Hou, C. W. Ashling, S. M. Collins, A. Krajnc, C. Zhou, L. Longley, D. N. Johnstone, P. A. Chater, S. Li, M. V. Coulet, P. L. Llewellyn, F. X. Coudert, D. A. Keen, P. A. Midgley, G. Mali, V. Chen and T. D. Bennett, *Nat. Commun.*, 2019, **10**, 1–10.
47 C. W. Ashling, D. N. Johnstone, R. N. Widmer, J. Hou, S. M. Collins, A. F. Sapnik, A. M. Bumstead, P. A. Midgley, P. A. Chater, D. A. Keen and T. D. Bennett, *J. Am. Chem. Soc.*, 2019, **141**, 15641–15648.
48 C. W. Ashling, L. K. Macreadie, T. J. F. Southern, Y. Zhang, L. N. McHugh, R. C. Evans, S. Kaskel, S. G. Telfer and T. D. Bennett, *J. Mater. Chem. A*, 2021, **9**, 8386–8393.
49 L. N. McHugh, M. F. Thorne, G. Robertson, G. Divitini and T. D. Bennett, *Chem. - Eur. J.*, 2022, **28**, 1–7.
50 D. S. Sholl and R. P. Lively, *Nature*, 2016, **532**, 435–437.
51 H. Fan, Y. Xie, J. Li, L. Zhang, Q. Zheng and G. Zhang, *J. Mater. Chem. A*, 2018, **6**, 17602–17611.
52 C. Algieri and E. Drioli, *Sep. Purif. Technol.*, 2022, **278**, 119295.
53 Z. Kang, H. Guo, L. Fan, G. Yang, Y. Feng, D. Sun and S. Mintova, *Chem. Soc. Rev.*, 2021, **50**, 1913–1944.
54 A. He, Z. Jiang, Y. Wu, H. Hussain, J. Rawle, M. E. Briggs, M. A. Little, A. G. Livingston and A. I. Cooper, *Nat. Mater.*, 2022, **21**, 463–470.
55 N. T. Tran, J. Kim and M. R. Othman, *Microporous Mesoporous Mater.*, 2019, **285**, 178–184.
56 Y. Zhao, Y. Wei, L. Lyu, Q. Hou, J. Caro and H. Wang, *J. Am. Chem. Soc.*, 2020, **142**, 20915–20919.
57 M. Hovestadt, S. Friebe, L. Helmich, M. Lange, J. Möllmer, R. Gläser, A. Mundstock and M. Hartmann, *Molecules*, 2018, **23**, 889.
58 A. K. Fard, G. McKay, A. Buekenhoudt, H. Al Sulaiti, F. Motmans, M. Khraisheh and M. Atieh, *Materials*, 2018, **11**, 74.
59 M. Ulbricht, *Curr. Opin. Chem. Eng.*, 2020, **28**, 60–65.
60 Z. X. Lu, A. Namboodiri and M. M. Collinson, *ACS Nano*, 2008, **2**, 993–999.
61 R. Müller, N. Anders, J. Titus and D. Enke, *Talanta*, 2013, **107**, 255–262.
62 A. P. Radlinski, M. Mastalerz, A. L. Hinde, M. Hainbuchner, H. Rauch, M. Baron, J. S. Lin, L. Fan and P. Thiyagarajan, *Int. J. Coal Geol.*, 2004, **59**, 245–271.
63 C. J. Jafta, A. Petzold, S. Risse, D. Clemens, D. Wallacher, G. Goerigk and M. Ballauff, *Carbon*, 2017, **123**, 440–447.